Regular Article

blood

LYMPHOID NEOPLASIA

Activating mutations in genes related to TCR signaling in angioimmunoblastic and other follicular helper T-cell–derived lymphomas

David Vallois,[1,*] Maria Pamela D. Dobay,[2,*] Ryan D. Morin,[3,4] François Lemonnier,[5] Edoardo Missiaglia,[1] Mélanie Juilland,[6] Justyna Iwaszkiewicz,[2] Virginie Fataccioli,[5] Bettina Bisig,[1] Annalisa Roberti,[1] Jasleen Grewal,[3] Julie Bruneau,[7] Bettina Fabiani,[8] Antoine Martin,[9] Christophe Bonnet,[10] Olivier Michielin,[2,11] Jean-Philippe Jais,[12] Martin Figeac,[13] Olivier A. Bernard,[14] Mauro Delorenzi,[2,11,15] Corinne Haioun,[16] Olivier Tournilhac,[17] Margot Thome,[6] Randy D. Gascoyne,[18] Philippe Gaulard,[5,†] and Laurence de Leval[1,†]

[1]Institute of Pathology, Centre Hospitalier Universitaire Vaudois, Lausanne, Switzerland; [2]SIB Swiss Institute of Bioinformatics, Lausanne, Switzerland; [3]Department of Molecular Biology and Biochemistry, Simon Fraser University, Burnaby, BC, Canada; [4]Genome Sciences Centre, BC Cancer Agency, Vancouver, BC, Canada; [5]INSERM U955, Université Paris-Est, Département de Pathologie, Hôpital Henri-Mondor, Créteil, France; [6]Department of Biochemistry, University of Lausanne, Lausanne, Switzerland; [7]Service d'Anatomie et cytologie pathologiques, Hôpital Necker, Paris, France; [8]Service d'Anatomie et cytologie pathologiques, Hôpital Saint-Antoine, Paris, France; [9]Service d'Anatomie pathologique, Hôpital Avicenne, Bobigny, France; [10]Hématologie clinique, CHU Liège, Liège, Belgium; [11]Department of Oncology, Centre Hospitalier Universitaire Vaudois, Lausanne, Switzerland; [12]Service de Biostatistiques, GH Necker-Enfants Malades, Paris, France; [13]Plate-forme de Génomique Fonctionnelle et Structurale, Institut Pour la Recherche sur le Cancer de Lille, Lille, France; [14]INSERM U1170, Institut Gustave Roussy, Villejuif, France; [15]Ludwig Center for Cancer Research, University of Lausanne, Epalinges, Switzerland; [16]Hémopathies lymphoides, CHU Henri Mondor, Creteil, France; [17]Hématologie Clinique, CHU Estaing, Clermont-Ferrand, France; and [18]Centre for Lymphoid Cancer, BC Cancer Agency, Vancouver, BC, Canada

Key Points

- A high frequency of diverse activating mutations in costimulatory/TCR-related signaling genes occurs in AITL and other TFH-derived PTCL.
- Deregulated TCR activation may play a role in the pathogenesis of TFH-derived PTCL, paving the way for developing novel targeted therapies.

Angioimmunoblastic T-cell lymphoma (AITL) and other lymphomas derived from follicular T-helper cells (TFH) represent a large proportion of peripheral T-cell lymphomas (PTCLs) with poorly understood pathogenesis and unfavorable treatment results. We investigated a series of 85 patients with AITL (n = 72) or other TFH-derived PTCL (n = 13) by targeted deep sequencing of a gene panel enriched in T-cell receptor (TCR) signaling elements. *RHOA* mutations were identified in 51 of 85 cases (60%) consisting of the highly recurrent dominant negative G17V variant in most cases and a novel K18N in 3 cases, the latter showing activating properties in in vitro assays. Moreover, half of the patients carried virtually mutually exclusive mutations in other TCR-related genes, most frequently in *PLCG1* (14.1%), *CD28* (9.4%, exclusively in AITL), *PI3K* elements (7%), *CTNNB1* (6%), and *GTF2I* (6%). Using in vitro assays in transfected cells, we demonstrated that 9 of 10 PLCG1 and 3 of 3 CARD11 variants induced MALT1 protease activity and increased transcription from NFAT or NF-κB response element reporters, respectively. Collectively, the vast majority of variants in TCR-related genes could be classified as gain-of-function. Accordingly, the samples with mutations in TCR-related genes other than *RHOA* had transcriptomic profiles enriched in signatures reflecting higher T-cell activation. Although no correlation with presenting clinical features nor significant impact on survival was observed, the presence of TCR-related mutations correlated with early disease progression. Thus, targeting of TCR-related events may hold promise for the treatment of TFH-derived lymphomas. (*Blood*. 2016;128(11):1490-1502)

Introduction

Angioimmunoblastic T-cell lymphoma (AITL), one of the most common peripheral T-cell lymphomas (PTCLs),[1,2] comprises $CD4^+$ neoplastic T cells with a T-follicular helper (TFH) immunophenotype, and an important reactive microenvironment.[3] In addition, a subset of PTCL not otherwise specified (PTCL-NOS) exhibiting a TFH-like immunophenotype and overlapping characteristics with AITL are believed to be part of the same disease spectrum.[4,5] The prognosis of AITL remains poor, with a 5-year overall survival of ~30%.[1,6] Although autologous stem cell transplantation may improve the response to conventional first-line therapy, early disease progression

Submitted February 18, 2016; accepted June 22, 2016. Prepublished online as *Blood* First Edition paper, July 1, 2016; DOI 10.1182/blood-2016-02-698977.

*D.V. and M.P.D.D. are considered co-first authors.

†P.G. and L.d.L. are considered co-last authors.

The online version of this article contains a data supplement.

There is an Inside *Blood* Commentary on this article in this issue.

The publication costs of this article were defrayed in part by page charge payment. Therefore, and solely to indicate this fact, this article is hereby marked "advertisement" in accordance with 18 USC section 1734.

makes it frequently impossible.[7] Thus, pinpointing new druggable targets for developing specific therapies in TFH-derived lymphomas remains critical.

Recurrent mutations in the epigenetic regulators *TET2*, *IDH2*, and *DNMT3A* have been detected in AITL and TFH-like PTCLs[8,9] but are not likely sufficient to drive lymphomagenesis.[10,11] A highly recurrent dominant-negative G17V mutation in the RHOA GTPase was recently discovered in as much as 70% of AITL and TFH-like PTCLs.[12-14] RHOA is activated downstream of T-cell receptor (TCR) engagement in mature T cells and is linked to cytoskeleton reorganization after T-cell activation.[12,13] Although their exact role in human T-cell transformation remains uncertain, *RHOA* mutations tend to co-occur with *TET2* mutations, suggesting that they represent a second event in multistep AITL lymphomagenesis.[15] Finally, AITL also bears a variety of other less recurrent genetic alterations.[12,13,16]

In B-cell lymphomas, constitutive B-cell receptor (BCR) signaling via somatic mutation-induced or antigen-mediated activation of key BCR components leads to neoplastic B-cell survival and expansion.[17] Several lines of evidence suggest that TCR activation might be similarly relevant to PTCL pathogenesis. For example, NPM1-ALK chimeric proteins induce an intracellular cascade of events substituting to TCR signaling in anaplastic large cell lymphoma.[18] The *ITK-SYK* fusion present in rare PTCLs likewise drives lymphomagenesis by triggering antigen-independent activation of TCR signaling pathways in mice.[19] Mutations or gene fusions in costimulatory/TCR signaling genes as *CD28, FYN, PLCG1*, or *CARD11* have also been reported in several PTCLs.[12,20-25] However, alterations in the TCR signaling pathway have not yet been extensively studied in TFH-related lymphomas. Here, we focused on investigating mutations in the costimulatory/TCR signaling cascade in a series of AITL and TFH-like PTCLs using a targeted deep-sequencing approach. Besides frequent RHOA mutations, we demonstrated recurrent activating and virtually mutually exclusive mutations in costimulatory/TCR pathway components in 49% of the cases. Notably, we found several mutations in *PLCG1* and *CARD11* that we characterized as functionally activating in vitro. Integrated analysis with gene expression profiles indicated that TCR-mutated samples were enriched for molecular signatures, reflecting higher T-cell activation and proliferation. Clinically, TCR-mutated patients receiving anthracyclin-based chemotherapy showed an increased early progression risk compared with patients without such mutations. These results indicate the potential of using drugs that reduce TCR signaling for treating these lymphomas.

Methods

Patients and tumor samples

Discovery cohort. Eleven paired tumoral and normal samples from 10 clinically annotated AITL patients were subject to whole-genome sequencing (WGS, n = 8) or whole-exome sequencing (WES, n = 3) (supplemental Table 1, available on the *Blood* Web site).

Extended cohort. Targeted deep sequencing (TDS) was performed on DNA extracted from frozen tissue biopsies of an extended cohort of 85 previously untreated patients (72 AITL, 13 TFH-like PTCL-NOS). In 3 patients, paired samples were analyzed. These cases and associated clinical annotations (supplemental Table 2) were collected in the framework of the Tenomic LYSA consortium. Diagnoses were confirmed by expert hematopathologists. Criteria used to define TFH-like PTCL-NOS were previously reported.[8] A subset of these patients was analyzed for *TET2, IDH2*, and *DNMT3A* mutations in previous studies.[8,9] The study was approved by the local ethics committee (CPP Ile de France IX 08-009).

WGS, WES, and TDS

Libraries were constructed for WGS following a standard protocol.[26] 100-bp paired-end reads were generated using an Illumina HiSequation 2000 Sequencer (version 3 chemistry). Reads were mapped to the NCBI Build 36.1 reference genome using the Burrows-Wheeler Aligner alignment tool version 0.5.7, algorithm aln. Polymerase chain reaction duplicates were eliminated using Picard version 1.38. Indels and single-nucleotide variants (SNVs) were called using Strelka version 1.0.14, removing false-positive calls internally. Variants were independently identified for each tumor-germline pair, using the germline as reference. GRCh37 coordinates of the filtered indels and SNVs were obtained using LiftOverVCF. Variants were annotated with VEP, and their read counts were obtained using in-house scripts. Copy number variations (CNVs) were identified using HMMcopy. Commonly deleted or amplified regions from WGS were visually identified using the Integrative Genome Viewer Software (IGV, https://www.broadinstitute.org/igv/). Deleted loci and genes having SNVs and/or CNVs in at least 2 patients are listed in supplemental Tables 3 and 4.

TDS of 69 genes (supplemental Table 5) was performed on the extended cohort. Systematic sequencing errors were removed by adding 2 randomly selected blood samples from 4 healthy volunteers to each run. Libraries were prepared using the True-Seq Custom Amplicon kit (Illumina) and sequenced on a MiSeq machine (Illumina, 1000× mean depth, mean coverage 94%). Variants were called using MiSeq reporter using default settings and were visually inspected on IGV. All synonymous variants and known SNPs with an allelic frequency >0.1% in public databases (dbSNP131, 1000 Genomes Project, 5000 Exomes project) were filtered out. We excluded variants found in normal samples, in ambiguously mapped regions from captured pseudogenes, and in regions of low complexity. Candidate variants were independently validated in a second round of TDS: we selectively amplified the amplicons covering the positions of candidate mutations (IonAmpliseq kit, Life Technologies) and sequenced them on an Ion PGM System (Life Technologies; 1305× mean depth, mean coverage 91.64%). Variants were called using default settings of the IonReporter software and reviewed with IGV. The final variants list (supplemental Table 6) was generated applying the following filtering criteria: (a) variants called by both platforms; (b) variants with minor allele frequency (MAF) <0.4; and (c) variants already described as somatic in the COSMIC database. Filter (b) was introduced to take into account the low tumor content and the unavailability of matched normal samples. The threshold was defined based on the MAF range of well-characterized AITL mutations, such as in *RHOA* and *CD28*.[12-14,25] Variants were annotated using GeneTalk (http://www.gene-talk.de/).

Cloning and functional validation

A detailed description is provided in the supplemental Material. Briefly, we performed site-directed mutagenesis of *RHOA*, *PLCG1*, and *CARD11* mutations on cloned cDNAs into pcMV6-MycFlag (*RHOA, PLCG1*) (Origene, C-terminal tag) and pcDNA3-HA (*CARD11*) (N-terminal tag)[27] vectors. RHOA variants were functionally assessed in vitro with rhotekin pull-down assays[12-14] and SRE (Serum Responsive Element) (Promega, Madison, WI) luciferase reporter assay using HEK293T cells.

PLCG1 and CARD11 variants were functionally tested by fluorescence resonance energy transfer (FRET)-based determination of their ability to induce MALT1 protease activity in HEK293T cells[28] and in luciferase-based assays using a NFAT reporter in HEK293T cells (forPLCG1) or a NF-κB reporter in Jurkat cells deficient in *CARD11*[29] (kindly provided by Dr. Xin Lin) (for CARD11) .

Western blot analysis

The following primary antibodies were used in western blotting: anti-HA (Covalab Biotechnology), anti-Myc (clone 4A6, Millipore), anti-CARD11 (clone 1D12, Cell Signaling), and anti-MALT1[28] and anti-Actin (ab3280, Abcam). Secondary antibodies were purchased from Jackson Laboratories.

Gene expression and enrichment analysis

Gene expression profiles generated by hybridization on Affymetrix U133 Plus 2.0 were available for the extended cohort.[3] Rotation testing using mean ranks

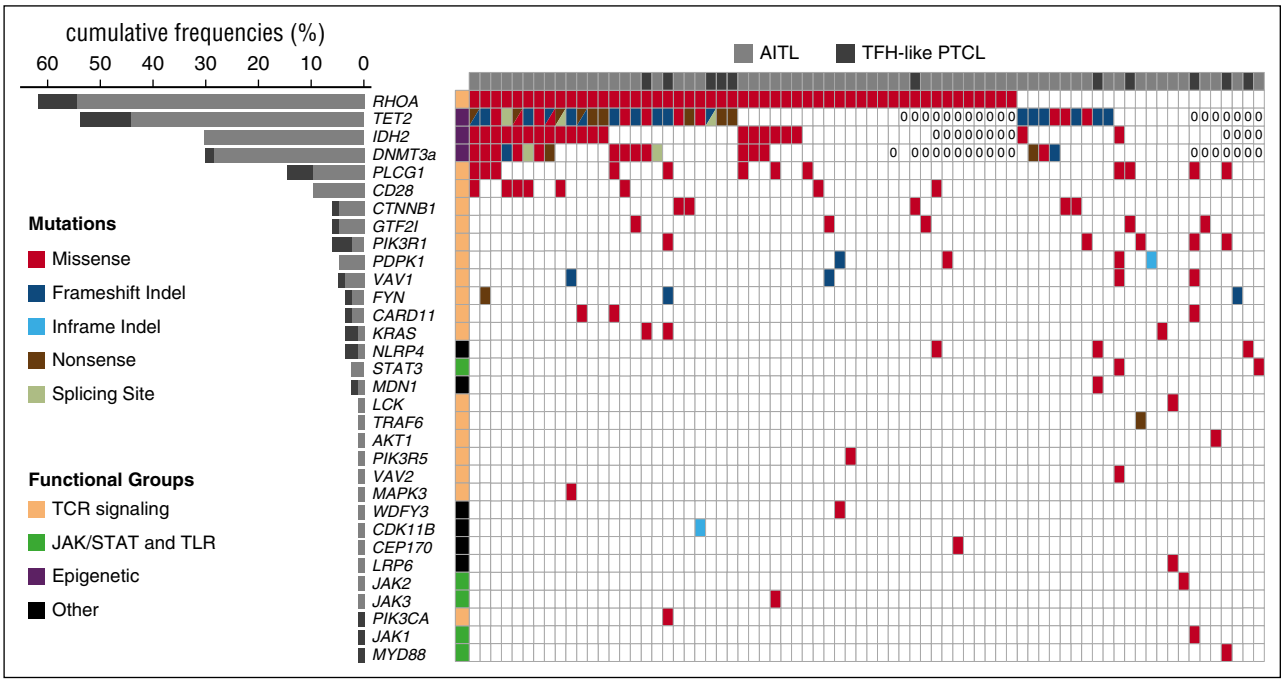

Figure 1. Mutational landscape of nodal TFH-derived lymphomas. The results of targeted deep sequencing of 69 genes in 72 AITL (light gray) and 13 TFH-like PTCL (dark gray) are presented. Ten cases (8 AITL and 2 TFH-like PTCL) with no mutations detected are not represented. *TET2, DNMT3A*, and *IDH2* mutations available for a subset of the cases reported in previous studies[8,9] are also shown. Case-mutation pairs for which data are not available are indicated by a 0. Mutated genes (rows) are arranged by decreasing order of mutation frequency. Patients (columns) are arranged from left to right based on their mutational status following gene ranking.

(ROMER, R package limma) was used to determine the gene set signature enrichments in TCR_Mut compared with TCR_WT patients. A total of 304 signatures, including 23 of 50 hallmark signatures and 9 signatures from the curated and immunogenic signature collection of the Molecular Signatures Database (MSigDB, http://software.broadinstitute.org/gsea/msigdb), all signatures of interest in lymphoid biology (Staudt, lymphochip.nih.gov/signaturedb/), and 2 manually annotated sequences linked to TCR signaling, were tested.

Clinical correlations and survival analysis

Frequency differences of categorical variables were analyzed using the Fisher exact test, whereas differences in continuous variables were tested with the Wilcoxon rank-sum test. Overall survival (OS) was defined as time from diagnosis to death or last follow-up, whereas progression-free survival (PFS) was defined as time from treatment initiation to death or progression or last follow-up. Analyses of OS and PFS were performed using the

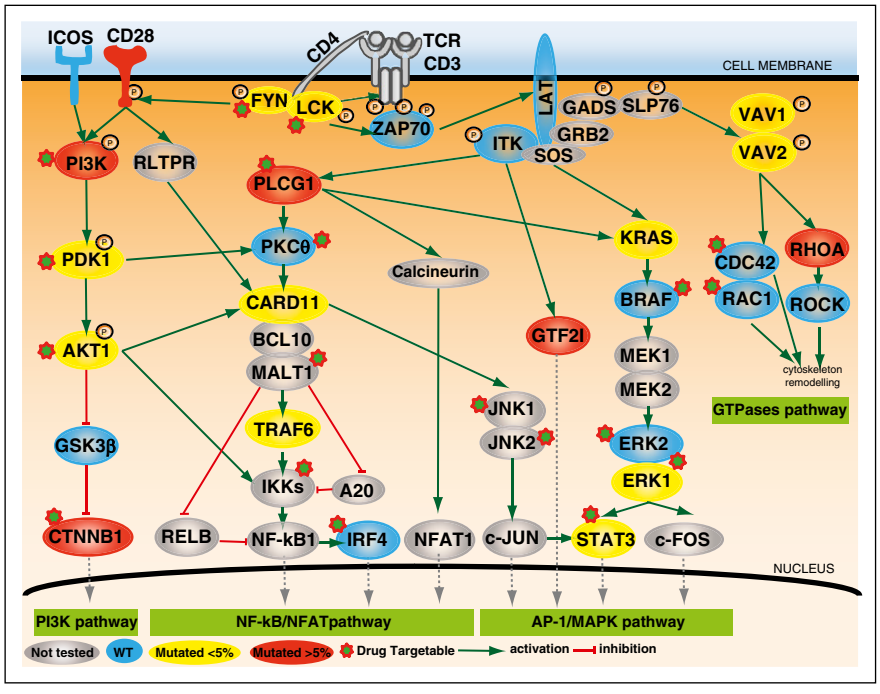

Figure 2. Mutations of TCR signaling–related genes in nodal lymphomas of TFH origin. The intracellular pathways after TCR ligation and costimulatory activation were reconstructed using the Ingenuity pathway analysis (IPA) tools, the KEGG database, and other references. Four main pathways are individualized, from left to right: (1) PI3K pathway after CD28/TCR-dependent FYN phosphorylation and ultimately resulting in CTNNB1 translocation into the nucleus; (2) NF-κB/NFAT pathway proximally initiated by ITK-dependent PLCG1 activation and resulting in NFAT1, NF-κB, and IRF4 activation; (3) AP-1/MAPK pathway that comprises ITK-dependent GTF2I activation, MALT1-induced JNKs activation, and PLCG1-GRB2/SOS–induced MAPK components activation; and (4) GTPase-dependent pathway, including RHOA, responsible for cytoskeleton remodeling upon costimulatory/TCR activation. The main positive interactions are indicated by solid green arrows, whereas inhibitory effects are indicated in red. The TCR signaling elements are depicted in yellow or red if the coding genes were mutated in <5% or ≥5% cases, respectively. The most frequently mutated genes (*PLCG1*, *CD28*, *PI3K* components, *CTNNB1*, and *GTF2I*) were part of costimulatory, NF-κB/NFAT, PI3K, and AP-1/MAPK intracellular signaling pathways. Proteins corresponding to WT genes are indicated in blue, and genes that were not sequenced are in gray. ERK1, ERK2, JNK1, JNK2, and PDK1 are protein names for *MAPK1, MAPK3, MAPK8, MAPK9*, and *PDPK1* genes, respectively.

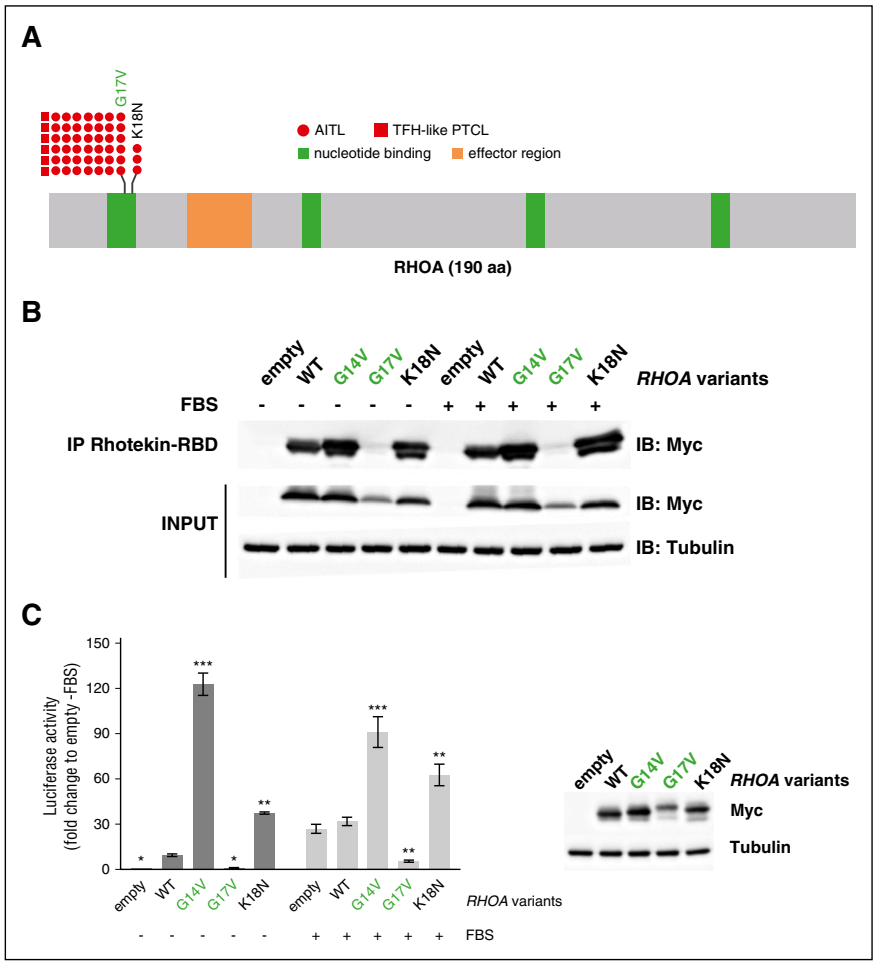

Figure 3. RHOA mutations in AITL and TFH-like PTCL. (A) Overview of the RHOA protein structure, showing G17V (42 AITL, 6 TFH-like PTCL) and the novel K18N (3 AITL) variants that target the highly conserved GTP/GDP binding site of RHOA. (B) Protein blot analysis of GTP-bound RHOA-Myc in rhotekin pull-down assay from HEK293T cells expressing indicated RHOA constructs. IP, immunoprecipitation. Representative of 6 independent experiments. (C) SRE (serum-responsive element) luciferase reporter assay monitoring the activity of RHOA K18N mutant, compared with WT, G14V, or G17V mutants, previously characterized as activating and dominant-negative, respectively. Cells were stimulated (light gray) or not (dark gray) with fetal bovine serum for 6 hours. Data are represented as mean ± standard error of the mean (SEM) from 4 independent experiments. Significant differences in activation activity were determined using 2-way analysis of variance (ANOVA) with repeated measurement (**$P \leq .01$; ***$P \leq .001$ compared with WT). Representative western blot from a luciferase assay experiment. Ectopic myc-tagged RHOA expression is revealed by anti-Myc. Anti-Actin blotting serves as loading control.

Kaplan-Meier method, and hazard ratio differences were computed with the log-rank test.

Results

Whole-exome/genome sequencing reveals alterations in T-cell signaling genes in AITL

Eleven tumor samples from 10 AITL patients were subject to WGS or WES and compared with germline DNA (supplemental Figure 1; supplemental Table 1). On average, 91% of the genome had >10× coverage, with 68% having >30×. A mean of 27 SNVs per patient (range 11-50) was observed in coding regions, except in a sample from a relapsing patient with a chromothripsis pattern of structural variation (supplemental Figure 2) and 225 SNVs. In one patient refractory to first-line therapy, WGS performed on tumor biopsies at diagnosis and after 5 cycles of chemotherapy revealed a similar profile of alterations, with identical *TET2* and *ANKRD62* SNVs in both samples. CNV analysis revealed multiple loci deleted in a number of patients, with 8 minimal common regions (supplemental Table 3), mostly in 3 patients. A total of 39 genes had SNVs and/or CNVs in at least 2 patients (supplemental Table 4). Apart from *RHOA* G17V and *TET2* mutations, 9 of 39 (23%) altered genes were related to TCR (n = 7), Toll-like receptor (n = 1), or Wnt (n = 1) signaling. Other mutations were found in genes involved in the cell cycle (n = 5), autophagy (n = 2), or other pathways (n = 6). Six additional genes relevant to TCR or JAK/STAT signaling (*CTNNB1, VAV1, MTOR, CREBBP, PIK3C2G, JAK1*) were altered in one patient each. Collectively, T-cell signaling alterations were found in 7 of 10 patients.

Frequent mutations of *RHOA* and other TCR-related genes are confirmed in an extended cohort of TFH-derived lymphomas

We designed a panel of 69 genes for TDS, partly based on findings in the discovery cohort (supplemental Table 5; supplemental Figure 1) for application on our extended cohort (supplemental Table 2). After orthogonal cross-validation and conservative filtering (supplemental Table 6; supplemental Figure 3), we validated 70 variants in 29 genes (Figure 1), including missenses (61), frameshifts (5), nonframeshift deletions (2), and stop-gain mutations (2). Mutations were detected in 70 of 85 samples (82%, mean mutations per sample = 1.8). *RHOA* and other TCR signaling–related genes accounted for 19 of 29 (65.5%) mutated genes (Figures 1 and 2).

RHOA mutations include a novel activating K18N variant

RHOA was the most frequently mutated gene among those analyzed (51/85; 60% of patients), with a similar prevalence in AITL and TFH-like PTCL. Consistent with previous reports,[12,13] the G17V variant was found in most of the cases. We also identified a novel K18N mutation (variant frequency [VF] [5.5%; 7.4%; 10%]) in 3 AITL patients (Figure 3A; Table 1).[30-44] Both mutations occur in the highly conserved GTP binding site of RHOA. We tested Myc-tagged

Table 1. Characteristics of the 70 variants identified by targeted deep sequencing of TCR, JAK/STAT, and TLR-related genes in 85 TFH-derived PTCL samples

Functional groups	Gene	Amino acid change	Mutation type	Domain	New/reported	Effect	References
Costimulatory and	*CD28*	D124V	Missense	Extracellular	AITL, ATLL	Gain of function (F)	20,25
proximal TCR	*CD28*	D124E	Missense	Extracellular	AITL, ATLL	Gain of function (F)	20,25
signaling	*CD28*	T195P	Missense	Cytoplasmic	AITL, ATLL	Gain of function (F)	20,25,30
	LCK	N446K*	Missense	Kinase	New	Probably gain of function (P)	
	LCK	P447R*	Missense	Kinase	New	Probably gain of function (P)	
	FYN	Q527X	Stop gain		ATLL	Probably gain of function (P)	20
	FYN	525_525del†	Frameshift deletion		New	Probably gain of function (P)	
	FYN	S186L†	Missense	SH2	New	Probably gain of function (P)	
	FYN	K108fs*	Frameshift deletion		New	Probably loss of function (P)	
	FYN	E107S*	Missense	SH3	New	Probably loss of function (P)	
NK-kB/NF-AT	*PLCG1*	E47K	Missense	PH 1	ATLL	Gain of function (F)	20
pathway	*PLCG1*	R48W	Missense	PH 1	ATLL, SS	No effect (F)	20,24
	PLCG1	D342G	Missense	PI-PLC X-box	ATLL, MF	Gain of function (F)	20
	PLCG1	S345F†	Missense	PI-PLC X-box	ATL, MF, SS, ATLL	Gain of function (F)	20-22,24
	PLCG1	S520F†	Missense	PH 2; first part	MF, SS, ATLL	Gain of function (F)	20,21,24
	PLCG1	E730K	Missense	SH2 2	New	Gain of function (F)	
	PLCG1	G869E	Missense	Near SH3	New	Gain of function (F)	
	PLCG1	E1163K	Missense	C2	ATLL, SS	Gain of function (F)	20,24
	PLCG1	D1165H	Missense	C2	ATLL, SS	Gain of function (F)	20,24
	PLCG1	D1165G	Missense	C2	ATLL	Gain of function (F)	20
	CARD11	F902C	Missense		ATLL	Gain of function (F)	20
	CARD11	S547T	Missense		New	Gain of function (F)	
	CARD11	F176C	Missense	Coiled coil	New	Gain of function (F)	
	TRAF6	Q347X	Stop gain	Coiled coil /MATH	New	NA	
PI3K pathway	*PIK3R1*	K141R	Missense	RHO-GAP	New	Probably gain of function (P)	
	PIK3R1	Q475P	Missense	iSH2	New	Probably gain of function (P)	
	PIK3R1	T576A	Missense	iSH2	New	Probably gain of function (P)	
	PIK3R1	G680S	Missense	SH2 2	New	Probably gain of function (P)	
	PIK3R1	V704M	Missense	SH2 2	New	Probably gain of function (P)	
	PIK3R5	A259V	Missense		Carcinoma (liver)	Probably gain of function (P)	31
	PIK3CA	L1001P	Missense	PI3K/PI4K	New	Probably gain of function (P)	
	PDPK1	19_20del	Inframe deletion		New	NA	
	PDPK1	151_152del	Frameshift deletion	Protein kinase	New	Probably loss of function (P)	
	PDPK1	R324Q	Missense	Protein kinase	New	Probably gain of function (P)	
	PDPK1	P340Q	Missense	Protein kinase	New	Probably gain of function (P)	
	AKT1	G294R	Missense	Protein kinase	New	Probably gain of function (P)	
	CTNNB1	T41A†	Missense	Phospho by GSK3b	Hepatocellular carcinoma, acute lymphoblastic leukemia, breast cancer, Wilms' tumor	Gain of function (F)	32
	CTNNB1	H36P	Missense		Hepatocellular carcinoma, acute lymphoblastic leukemia, breast cancer, Wilms' tumor	Gain of function (F)	32
	CTNNB1	S45F†	Missense		Hepatocellular carcinoma, acute lymphoblastic leukemia, breast cancer, Wilms' tumor	Gain of function (F)	32
	CTNNB1	K335T	Missense		Hepatocellular carcinoma	Gain of function (F)	33

Genes are organized by functional groups.
AITL, angioimmunoblastic T-cell lymphoma; ATLL, adult T-cell lymphoma/leukemia; DLBCL, diffuse large B-cell lymphoma; F, functional validation; MF, mycosis fungoides; P, literature- and models-based; SS, Sézary syndrome.
*Gene variants found in the same patient and in the same allele.
†Gene variants found in the same patient but in different alleles.

Table 1. (continued)

Functional groups	Gene	Amino acid change	Mutation type	Domain	New/reported	Effect	References
AP-1/MAPK	*KRAS*	I36M	Missense		Hematopoeitic neoplasms	Gain of function (F)	34
pathway	*KRAS*	A18D	Missense	GTP binding	Lymphoma	Gain of function (F)	34
	KRAS	G13D	Missense	GTP binding	Solid tumors	Gain of function (F)	34
	MAPK3	R278Q	Missense	Protein kinase	New	Probably gain of function (P)	
	STAT3	E616G	Missense	SH2	Lymphoma	Gain of function (F)	26,35
	STAT3	E616K	Missense	SH2	Lymphoma	Gain of function (F)	26,35
	GTF2I	D317E	Missense		New	Probably gain of function (P)	
	GTF2I	N340S	Missense		New	Probably gain of function (P)	
	GTF2I	R523S	Missense	GTF2I-like	New	Probably gain of function (P)	
	GTF2I	L607F	Missense	GTF2I-like	New	Probably gain of function (P)	
	GTF2I	R702Q	Missense		New	Probably gain of function (P)	
GTPases	*RHOA*	K18N	Missense	GTP binding	New	Gain of function (F)	
pathway	*RHOA*	G17V	Missense	GTP binding	AITL, ATLL	Dominant negative (F)	12-14,20,36
	VAV1	151_158del	Frameshift deletion		New	Probably loss of function (P)	
	VAV1	778_783del	Frameshift deletion		New	Probably gain of function (P)	
	VAV1	D797G	Missense	SH3 2	New	Probably gain of function (P)	
	VAV1	Y826S	Missense	SH3 2	New	Probably gain of function (P)	
	VAV2	Y214C	Missense	DH	Gastric carcinoma	Probably dominant negative (P)	
JAK/STAT and	*JAK1*	D831E	Missense	Kinase	New	Probably gain of function (P)	
TLR pathways	*JAK2*	V617F	Missense		Myeloproliferative disorders	Gain of function (F)	37-43
	JAK3	A699V	Missense	Kinase	Lymphoma, carcinoma	Gain of function (F)	37-43
	MYD88	S219C	Missense	TIR	DLBCL, lymphocytic leukemia	Probably gain of function (P)	44

Genes are organized by functional groups.
AITL, angioimmunoblastic T-cell lymphoma; ATLL, adult T-cell lymphoma/leukemia; DLBCL, diffuse large B-cell lymphoma; F, functional validation; MF, mycosis fungoides; P, literature- and models-based; SS, Sézary syndrome.
*Gene variants found in the same patient and in the same allele.
†Gene variants found in the same patient but in different alleles.

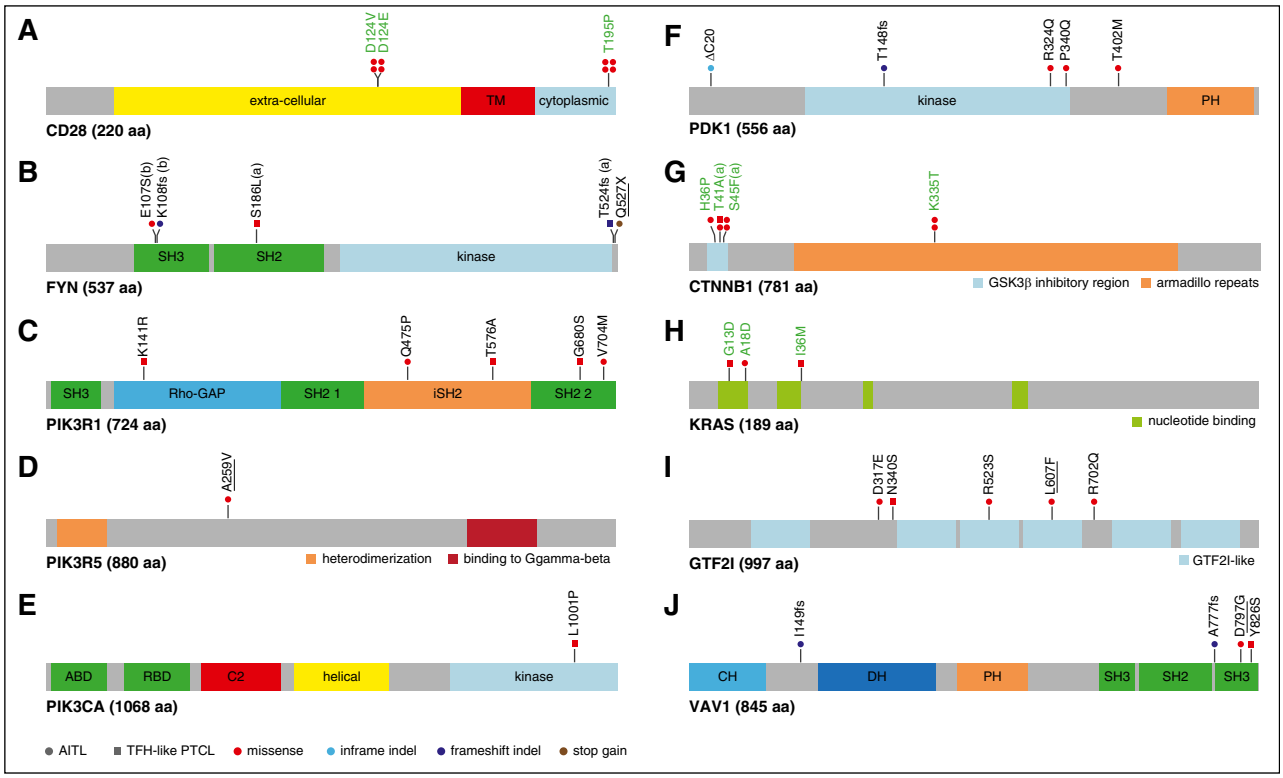

Figure 4. Mapping of variants in TCR signaling genes mutated in at least 3 patients. (A) CD28: the D124V/E variants involve the extracellular part of the receptor, whereas T195P lies in the intracellular, C-terminal, domain between the 2 domains, allowing interaction with PIK3R1 (YVKM sequence) or GRB2/VAV (PRRP sequence) proteins. (B) FYN: the five mutations indicated occurred in three patients; 1 patient harbored 2 mutations (a); 2 mutations in adjacent positions in the SH3 domain (b) were observed on the same allele in another patient. (C-E) PI3K subunits: when appropriate, cellular stimuli are present, the nSH2 and cSH2 domains of PIK3R1 bind phosphorylated tyrosines (YXXM motif) in activated receptors (CD28) and adapter proteins, thereby activating the PIK3CA (p110a) catalytic subunit without releasing the PIK3R1 (p85a) interaction with p110a through their iSH2 and ABD domains, respectively. The K141R missense affects the ρ-GAP domain, whereas iSH2 and the second SH2 domains of PIK3R1 bore 2 missenses each (Q475P, T576A and G680S, V704M, respectively). The A259V mutation, described as somatic in COSMIC, affects a linker region of PIK3R5. Finally, the L1001P point mutation affects the PIK3CA kinase domain. (F) PDK1: one inframe INDEL, one frameshift INDEL, and 3 missense affect PDK1 protein. (G) CTNNB1: 3 previously described activating missenses affect the GSK3β inhibitory domain (exon 3), whereas the K335T activating mutation affects the armadillo repeats region. (H) KRAS: 3 missense mutations alter 2 N-terminal nucleotide binding regions. (I) GTF2I: 5 missense mutations affect the GTF2I transcription factor, among which two are found in different GTF2I-like domains. (J) VAV1: 2 frameshift deletions and 2 missenses affect VAV1, three being localized in the C-terminal SH3 domain of the protein. In all figure panels, previously described activating mutations are in green boldface, and mutations previously described but not functionally tested are underlined. PDK1 is the protein name of *PDPK1* gene.

G14V (constitutively active[45]), G17V (dominant-negative), K18N, and wild-type (WT) RHOA in a pull-down assay using Rhotekin-RBD (ρ binding domain) beads (Figure 3B). Although RHOA G17V already characterized as dominant-negative[12-14] did not bind RBD beads, even in the presence of fetal bovine serum, compared with WT, RHOA K18N showed a marked increase of RBD beads binding similarly to RHOA G14V (Figure 3B). Moreover, unlike RHOA G17V that did not activate and even repressed transcription from the SRE under serum activation, RHOA K18N markedly enhanced its transcription (Figure 3C).

Mutations in other TCR signaling–related genes are variably recurrent and diverse

Apart from *RHOA*, mutations in genes involved in TCR costimulation or signaling were detected in 42 of 85 patients (49%) (Figures 1 and 2; Table 1).

CD28 and TCR-proximal signaling genes. Three different *CD28* mutations—T195P, D124V, and D124E—all described previously[13,25,30] were identified in 4, 2, and 2 AITL patients, respectively (8/85, 9.4%) (Figure 4A). All TFH-like PTCL were *CD28*-WT. T195P and D124V mutations are known to enhance TCR/CD28-induced NF-κB activity in vitro.[25,30] Three patients (2 AITL, 1 TFH-like PTCL; 3.5%) harbored mutations in *FYN*, a TCR- and CD28-proximal kinase component (Figure 4B). Mutations in the SH2 domain (S186L) and the absence of phosphorylated tyrosine 531 (T524fs or Q527X mutations) probably confer enhanced kinase activity by disrupting their inhibitory interaction.[12] The 2 amino acid substitutions in the tyrosine kinase domain of LCK observed in one AITL patient is expected to enhance its kinase activity.[46] We did not find mutations in *ICOS, ZAP70, LAT*, or *ITK*.

NF-κB/NFAT pathway. Ten different missense mutations spanning the coding region of *PLCG1* (VF [2.1%; 38%]) were identified in 12 of 85 patients (8 AITL, 4 TFH-like PTCL; 14.1%) (Figure 5A). Apart from previously reported variants in adult T-cell leukemia/lymphoma (ATLL) or in other PTCL,[20-24] we identified 2 novel variants (E730K and G869E). We generated all mutant constructs and tested their activity against WT PLCG1 in a FRET-based reporter assay of MALT1 protease activity[27,28] (Figure 5B) and in a NFAT luciferase reporter assay (Figure 5C). Both experiments confirmed that the S345F and S520F variants were activating.[21] All 6 variants in the PI-PLC, SH2, SH3, and C2 domains were also activating, increasing the FRET signal by 1.7- to threefold and the luciferase expression by four- to fivefold. Of the 2 PH1 domain variants, R48W had no effect in both assays, whereas E47K increased NFAT reporter activity by 2.1-fold and FRET signal by 1.5-fold.

Point mutations in *CARD11*, which encodes a scaffolding protein downstream of PLCG1 required for CD28/TCR-induced NF-κB

activation,[28] were found in 2 AITL and 1 TFH-like PTCL (3.5%). The F176C variant affects the coiled-coil domain of the protein, commonly mutated in diffuse large B-cell lymphoma (DLBCL).[27] The S547T and F902C variants map to linker regions with undefined structure (Figure 5D). In a FRET-based assay,[28] F176C and S547T enhanced MALT1 proteolytic activity by two- and fourfold, respectively, whereas the F902C mutant, previously reported in ATLL patients,[20] had no detectable effect (Figure 5E). When transfected into Jurkat cells deficient for *CARD11*,[29] we found that, compared with WT CARD11, all 3 variants induced enhanced NF-κB reporter activity in response to phorbol myristate acetate/ionomycin stimulation (Figure 5F).

PI3K pathway. Six patients (3 AITL, 3 TFH-like PTCL; 7%) showed mutations in *PI3K* genes encoding the regulatory subunits PIK3R1 (n = 5), PIK3R5 (n = 1), or the catalytic subunit PIK3CA (n = 1) (Figure 4C-E). These mutations likely enhance the catalytic subunit activity or increase PIK3R1 binding to CD28.[31] Five AITL patients (5.9%) had mutations in *PDPK1* (PDK1), a master serine/threonine kinase with multiple targets including AKT. Three missense mutations were found on or near its kinase domain, suggesting an activating effect[47] (Figure 4F). Four different *CTNNB1* mutations, known to occur in a variety of carcinomas and Wilms' tumors, were identified in 5 patients (4 AITL, 1 TFH-like PTCL; 5.9%) (Figure 4G). All have been previously characterized as activating or stabilizing variants that induce persistent signaling and increased proliferation, and have been linked to both poor treatment response and frequent tumor relapse in various tumors.[32,33]

AP-1/MAPK pathway. Eleven patients (8 AITL, 3 TFH-like PTCL; 13%) had mutually exclusive activating mutations in the MAPK pathway, which regulate the activity of the AP-1 transcription factor family. Activating *KRAS*[34] and *STAT3*[26,35] mutations were detected in 3 and 2 patients, respectively (Figure 4H). We also found 5 missense mutations in *GTF2I* (*TFII-I*)[48] (Figure 4I), which are likely activating as those reported in thymic epithelial tumors.[49]

GTPases pathway. Apart from highly recurrent *RHOA* mutations, 4 patients (3 AITL, 1 TFH-like PTCL; 4.7%) harbored previously undescribed frameshift deletions or missense mutations in *VAV1,* a guanosine exchange factor for RAC1, CDC42, and RHOA (Figure 4J). Two missense mutations were on the second SH3 domain, where a D797 residue mutation was previously shown to activate VAV1-mediated transformation via cell-cell contact deregulation.[50]

Analysis of sequential biopsies. Analysis of paired samples in 4 refractory or relapsed patients (supplemental Table 8) showed that the mutations identified at diagnosis were also present in the second biopsy, with overall very similar VF. Within the limit of the panel of genes examined, 2 patients presented one additional mutation at relapse (*CTNNB1* and *VAV1*), at somewhat lower VF than those present at diagnosis. Although this analysis is limited to a few pairs of samples, it indicates that the mutational heterogeneity that characterizes many AITL samples appears to be preserved and is essentially not modified by the treatments administered.

Activating mutations in TCR signaling–related genes correlate with molecular signatures reflecting higher T-cell activation and with response to therapy

Sixty-six of 85 patients harbored mutations in TCR signaling genes. To assess the biological and clinical impact of the tumor mutational status, we focused on patients with mutations in TCR signaling–related genes other than *RHOA,* designated hereafter as "TCR_Mut" (42/85 cases, 49%), and compared them with those with only *RHOA* or no detectable mutation, designated "TCR_WT" (43/85 cases, 51%) (Figure 6).

Mutations in TCR-related genes other than *RHOA* were virtually nonoverlapping, and the vast majority (47/56 distinct variants, 84%) were either functionally validated (n = 24) or predicted (n = 23) to be biologically gain-of-function mutants (Figure 6). Consequently, nearly all TCR_Mut patients (39/42 patients, 93%) harbored at least 1 activating mutation.

There were no significantly differentially expressed genes between TCR_Mut and TCR_WT samples (supplemental Figure 4). However, the molecular signatures of TCR_Mut were significantly enriched in 15 gene sets compared with TCR_WT by enrichment analysis (Figure 7A; supplemental Table 7; supplemental Figure 5), reflecting the activation of signaling pathways like PI3K, NF-κB,[17] IRF4, and JAK-STAT, as well as the upregulation of calcium-signaling target genes. This points toward TCR signaling activation in TCR_Mut PTCLs. TCR_Mut samples also showed enrichment in cell-cycle signatures reflecting increased proliferative activity. Finally, there was a trend for TCR_Mut samples to have downregulated proximal TCR signaling genes (signature "T_cell") such as TCR (*TCRα, TCRβ; CD3δ, CD3γ*), signaling molecules (*LAT, TRIM, SAP, FYB, ZAP70*), and cell surface markers (adjusted $P = .10$), a feature consistent with sustained T-cell activation.[51]

Then, when comparing the clinical features and outcome of TCR_Mut and TCR_WT patients, no significant differences in main clinical characteristics at presentation (supplemental Table 9) or in OS (18 vs 40 months median OS; 5-year OS 20% vs 29%; $P = .37$) were found (supplemental Figure 6). Strikingly, however, among the 59 patients (49 AITL and 10 TFH-like PTCLs) who received anthracyclin-based induction chemotherapy, 11 of 33 (33%) TCR_Mut patients vs 2 of 26 (8%) TCR_WT ($P = .02$, supplemental Table 9) showed early progression, relapse, or no response to treatment within the first 6 months after diagnosis. This, however, did not translate into a statistically significant difference in PFS at 5 years (21% vs 24% for TCR_Mut vs TCR_WT patients; $P = .15$) (Figure 7B-C).

Discussion

In this study, we confirmed the high prevalence of *RHOA* mutations in TFH-derived PTCL, with most samples bearing the dominant-negative G17V variant. Interestingly, we identified a new K18N variant in 3% of the patients that presented activating features in in vitro assays. This intriguing finding of distinct *RHOA* mutations, with apparently opposite functional properties in the same disease, was also recently documented in ATLL.[36,52] Further studies are warranted to understand how these variants may contribute to the pathogenesis of PTCLs.

Apart from *RHOA* alterations, we identified activating and virtually mutually exclusive mutations in diverse TCR signaling genes in half of TFH-derived lymphomas. Individually, the frequencies of these mutations were variable, with the 5 most mutated genes (*PLCG1, CD28, PIK3* elements, *GTF2I*, *CTNNB1)* being altered in 14% to 5% of the patients. *CD28* and *FYN* mutations in AITL were previously described in a small number of cases.[12-14] Our study significantly expands these previous results and strongly supports a role of activated TCR signaling in the pathogenesis of TFH-derived PTCLs, drawing strong parallels with the role of BCR signaling in B-cell lymphomas.

Mutations in genes related to TCR costimulation and signaling were recently reported in other PTCL entities, like cutaneous T-cell lymphomas, PTCL-NOS, and ATLL.[20-24,53] Nonetheless, mutations in specific genes are variably recurrent in distinct entites,[24,25] and for a given gene, the distribution of the mutations and their relative prevalence are

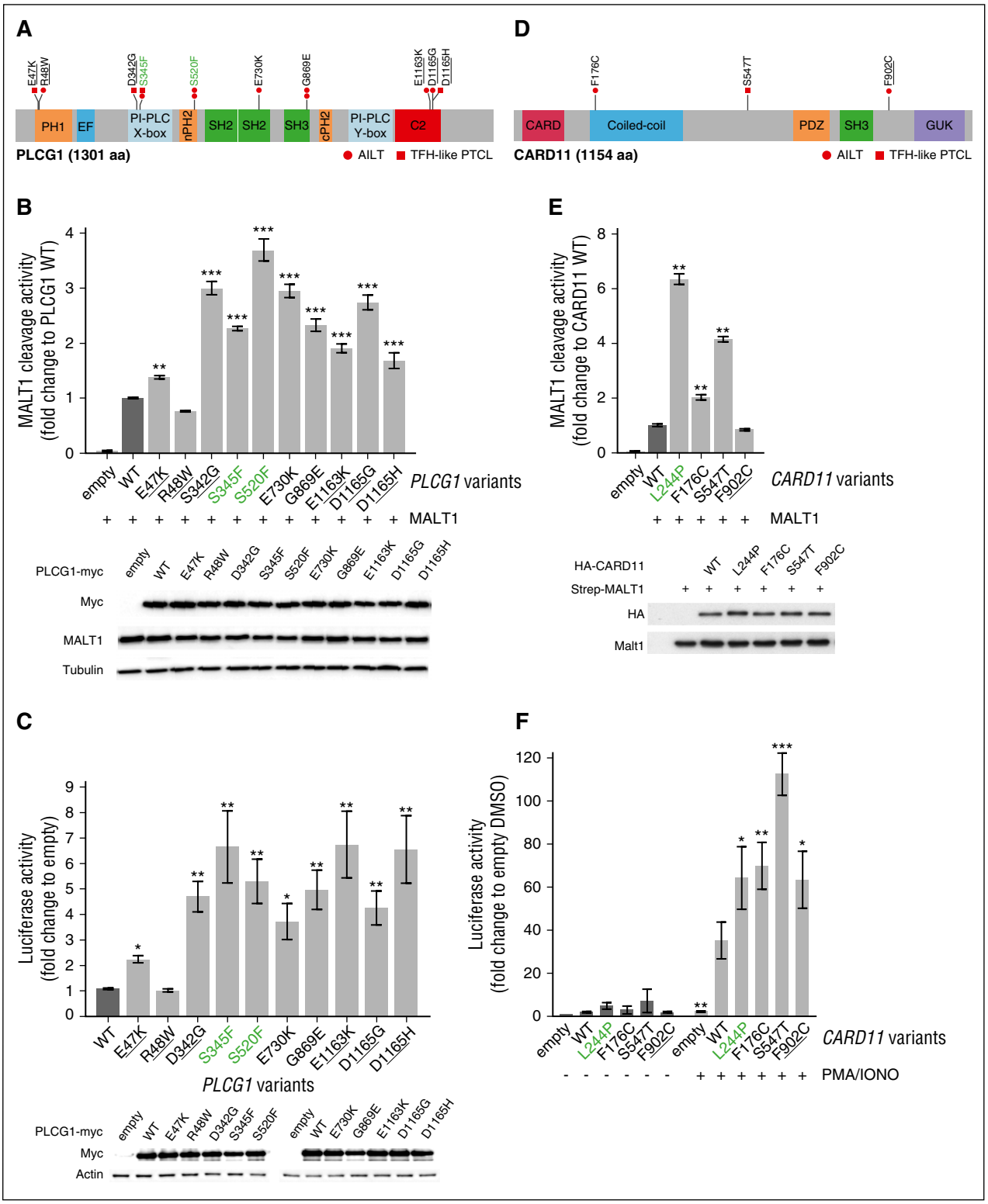

Figure 5. Mapping and functional analysis of PLCG1 variants and CARD11 variants. (A) Schematic representation of PLCG1 protein with mapping of the 10 missense mutations identified in AITL (circles) or TFH-like PTCL (squares) cases. Previously described activating mutations are in green boldface and mutations previously described but not functionally tested are underlined. (B) Monitoring of PLCG1-mediated MALT1 activation via a FRET-based reporter assay. Data are represented as mean ± SEM from 3 independent experiments. Significant differences in activation activity were determined using 1-way ANOVA (**$P \leq .01$; ***$P \leq .001$). Representative western blot from a MALT1 activation experiment. PLCG1 expression is revealed by anti-Myc tag blotting, whereas MALT1 expression is shown by anti-MALT1 antibody. (C) NFAT luciferase reporter assay monitoring activity of PLCG1 mutants, compared with previously reported activating mutants (green). Data are represented as mean ± SEM from 7 independent experiments. Significant differences in activation activity were determined using 1-way ANOVA (*$P \leq .05$; **$P \leq .01$). Representative western blot from a luciferase assay experiment. Ectopic myc-tagged PLCG1 expression is revealed by anti-Myc. Anti-Actin blotting serves as loading control. (D) Schematic representation of CARD11 protein with mapping of the 3-point mutations found in 2 AITL (circles) and 1 TFH-like PTCL-NOS (square) patients. A previously described mutation is underlined. (E) Monitoring of CARD11-mediated MALT1 activation via a FRET-based reporter assay. Data are

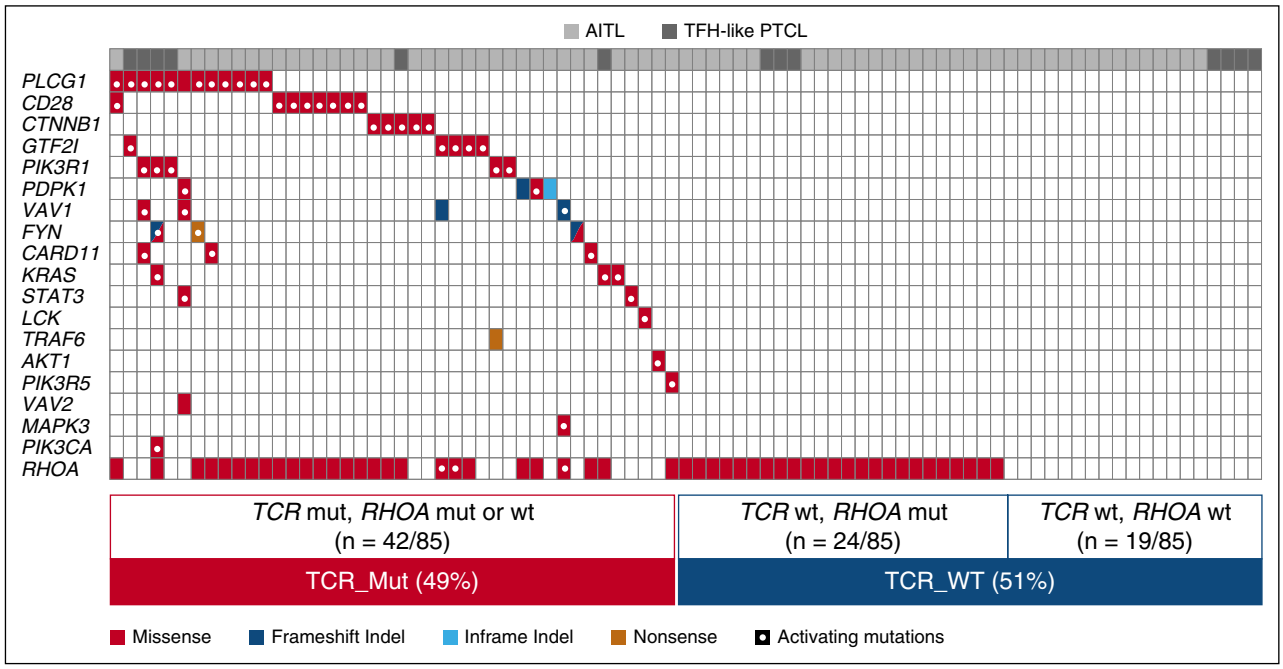

Figure 6. Mutual exclusivity of TCR signaling variants. The mutational status of TCR-related genes is represented for the 85 patients of the extended cohort. Genes other than *RHOA* are ranked by decreasing mutation frequency and show an essentially mutually exclusive mutation pattern. In total, 49% of cases were mutated in 1 or several TCR-related gene(s) other than *RHOA* (hereafter considered as TCR_Mut), 28.5% were mutated in *RHOA* only, and 22.5% harbored no mutation in any of the genes tested (collectively considered as TCR_WT).

heterogeneous. For instance, *PLCG1* and *CARD11* mutations are highly prevalent (up to 18% and 15% of the cases, respectively) in cutaneous T-cell lymphoma, in which conversely *CD28* mutations are not found.[20] *CARD11* mutations are more frequent in ATLL (24%) and Sézary syndrome (10.9%) than in this series of TFH-derived lymphomas. Whether the observed mutations are sufficient to induce constitutive activation of the respective pathways, and how their effect may be dependent or influenced by antigen-driven or other stimulatory signals remains unknown. Interestingly, some of the TCR-related genes may be altered through point mutations or small indels as well as by major structural rearrangements, amplifications, and deletions.[20,23,24] Collectively, these findings strongly suggest that genetic alterations affecting TCR signaling operate as a common pathogenic mechanism in several PTCL entities.

Our analysis also explored the JAK/STAT and TLR pathways. Mutation-induced activation of the JAK/STAT pathway, highly prevalent in myeloid neoplasms, was recently identified as a major oncogenic mechanism in several T-cell leukemias and lymphomas derived from innate immune cells.[20,37-43,53] Our results suggest, however, that JAK/STAT mutations do not have the same importance in the pathogenesis of TFH-derived lymphomas, because only 4 of 85 patients bore a single activating mutation each in *JAK1*, *JAK2, JAK3*, or *MYD88* (Table 1).[44] Except for *JAK2* V617F, the 3 others were observed in *PLCG1*-mutated cases.

Our data further support that AITL and TFH-like PTCL are closely related at the molecular level[5] and share common oncogenic mechanisms. We and others have reported the occurrence of *TET2*, *DNMT3A*, and *RHOA* mutations in a large proportion of both AITL and TFH-like PTCL patients.[5,8,9,12-14] This study extends the molecular overlap across TFH-derived neoplasms to genetic alterations in various TCR-signaling. Interestingly, *CD28* mutations were exclusively identified in AITL patients, consistent with recent reports.[25,30] Similarly, *IDH2* mutations were rarely detected in PTCL cases,[9,54] suggesting that the distribution of some genetic features might be relevant in distinguishing AITL from other TFH-derived nodal lymphomas, which otherwise share many common features.[5]

In the proposed multistep model of pathogenesis for TFH-derived PTCL, mutation-induced epigenetic deregulation, possibly arising in early hematopoietic precursors, may promote the emergence of premalignant cells, which requires additional genetic events to acquire a definitively malignant phenotype.[13,55] It has been thus suggested that *RHOA* alterations occur as a second event in *TET2*- and/or *DNMT3A*-mutated cells.[13,55,56] The prevalence of mutations in *TET2, DNMT3A*, and *IDH2* analyzed in a subset of our cases was 52% (34/65 cases), 29% (17/56 cases), and 30% (21/71 cases), respectively.[8,9] These mutations were not mutually exclusive, and in fact tended to co-occur with each other, as previously reported.[12,13] We also found a tendency for *RHOA* mutations to associate with epigenetic alterations, because *RHOA* mutations were detected in 31 of 41 (76%) cases mutated in *TET2*, *DNMT3A*, and/or *IDH2,* but in only 8 of 23 (35%) cases without epigenetic mutations ($P = .003$). Because the proportion of neoplastic cells in AITL is typically low and variable from case to case,[3] the comparison of VF of different

Figure 5 (continued) represented as mean ± SEM from 6 independent experiments. Significant differences in activation activity were determined using 1-way ANOVA (*$P \leq .05$; **$P \leq .01$). The known activating L244P variant (green) was used as a positive control for the experiment. Representative western blot from a MALT1 activation experiment. CARD11 expression is revealed by anti-HA tag blotting, whereas MALT1 expression is shown by anti-MALT1 antibody. (F) NF-κB luciferase reporter assay in Jurkat cells deficient for *CARD11* monitoring activity of CARD11 mutants, compared with previously reported activating mutants (green). Data are represented as mean ± SEM from 4 independent experiments. Significant differences in activation activity were determined using 2-way ANOVA (*$P \leq .05$; **$P \leq .01$; ***$P \leq .001$ compared with WT PMA/IONO).

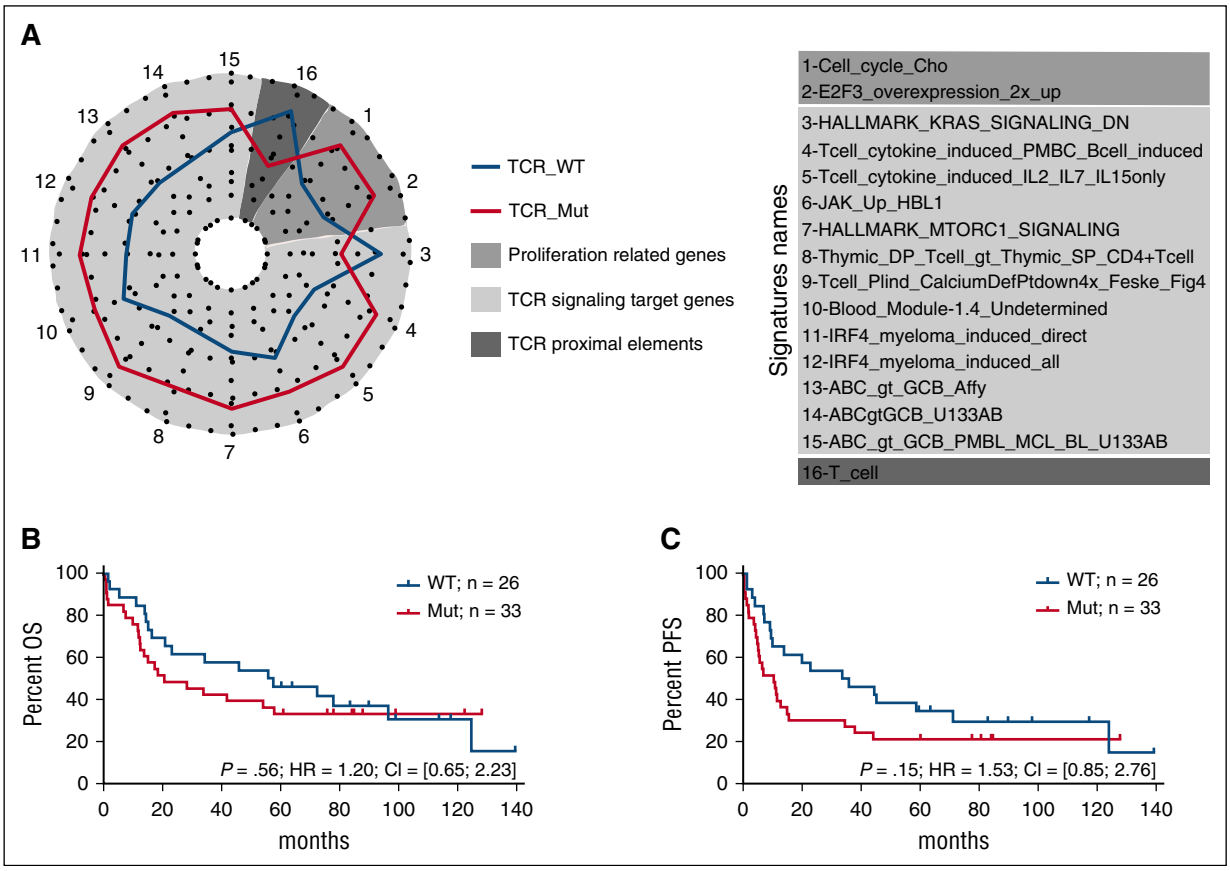

Figure 7. Biological significance and clinical relevance of TCR signaling–related mutations. (A) Spider plot representation of gene sets differentially enriched in patients with or without mutations in genes related to TCR signaling (TCR_Mut vs TCR_WT). Genes tested in the enrichment analysis were selected from signatures relevant in T- and B-cell differentiation and activation. Statistical significance of the enrichment was reached for gene sets 1 to 15 ($P < .05$); for gene set 16, marginal significance was observed ($P = .1$). (B-C) Overall survival (B) and progression-free survival (C) of patients with (red) or without (blue) mutations in TCR signaling–related genes. Analyses are restricted to the 59 patients treated with anthracyclin-based chemotherapy. Mutated patients show a trend toward a shorter PFS (11 vs 36 months) than WT patients ($P = .15$).

mutated genes was performed for each individual sample. In 13 cases harboring mutations in both *TET2* and/or *DNMT3*, and *RHOA* or *IDH2* with available VF, the *TET2/DNMT3A* VF was significantly higher than for *RHOA* or *IDH2* (supplemental Figure 7A). There was no obvious association of *RHOA* mutations with other TCR-related genes, because 27 of 51 (53%) *RHOA*-mutated and 15 of 34 (44%) *RHOA*-WT cases were mutated in other TCR-related genes ($P = .51$). In 27 cases mutated in both *RHOA* and one or several genes of the TCR, JAK/STAT, or TLR pathways, no significant difference in VF means was observed between *RHOA* and other genes (supplemental Figure 7B).

Although our results warrant confirmation in cohorts of patients treated on prospective clinical trials, they suggest that the mutational status of TCR-related genes may have important clinical implications, predicting early treatment failure with anthracyclin-based chemotherapy in TFH-related PTCL patients. Importantly, several activating mutations found in PI3K or NF-κB pathways could be targeted by idelalisib or the proteasome inhibitor bortezomib, respectively. It is of interest to determine their efficacy in TCR_Mut patients,[12,21] possibly in combination with demethylating agents.[57] Thus, similar to the importance of targeting BCR signaling in B-cell lymphomas with the BTK inhibitor ibrutinib,[17] characterization of the TCR mutational status might open new avenues to design specific and more effective therapies. In clinical practice, given the high number of genes involved and the diversity of mutations found, targeted deep sequencing with high depth/coverage appears to be the method of choice for selecting patients.

Acknowledgments

The authors acknowledge Catherine Chapuis (Pathology, Lausanne) and Caroline Communaux from the LYSA-Pathology for their technical assistance; K. Harshman and the Lausanne Genomic Technology Facility for their technical support; and Céline Villenet and Sabine Quief from the plate-forme de génomique fonctionnelle et structurale, Lille University, for the WES experiments.

This study was supported by grants received from the Plan Cancer (Belgium), the Ligue du Cancer (Switzerland), the Institut National du Cancer (INCa AAP PLBIO13-085, INCa-DGOS 2010-085, and INCa-Plan Cancer 2013), and the MEDIC foundation.

Authorship

Contribution: D.V., R.D.M., M.T., R.D.G., L.d.L., and P.G. conceived and designed the study; D.V. and M.P.D.D. developed the methodologies; D.V., M.P.D.D., J.B., B.F., A.M., C.B., F.L., M.J., M.T., J.I., A.R., M.F., and B.B., acquired the data; D.V., M.P.D.D., E.M., F.L., M.J., O.M., O.T., C.H., M.D., O.A.B., J.-P.J., and J.G. analyzed and interpreted the data; D.V., M.P.D.D., F.L., E.M., L.d.L.,

and P.G. wrote the manuscript; V.F. was the administrative, technical, and material support; and L.d.L. and P.G. supervised the study.

Conflict-of-interest disclosure: The authors declare no competing financial interests.

ORCID profiles: D.V., 0000-0003-0703-6762.

Correspondence: Laurence de Leval, CHUV Institut de Pathologie, Rue du Bugnon 25, 1011 Lausanne, Switzerland; e-mail: laurence.deleval@chuv.ch.

References

1. Federico M, Rudiger T, Bellei M, et al. Clinicopathologic characteristics of angioimmunoblastic T-cell lymphoma: analysis of the international peripheral T-cell lymphoma project. *J Clin Oncol.* 2013;31(2):240-246.
2. de Leval L, Parrens M, Le Bras F, et al. Angioimmunoblastic T-cell lymphoma is the most common T-cell lymphoma in two distinct French information data sets. *Haematologica.* 2015;100(9):e361-e364.
3. de Leval L, Rickman DS, Thielen C, et al. The gene expression profile of nodal peripheral T-cell lymphoma demonstrates a molecular link between angioimmunoblastic T-cell lymphoma (AITL) and follicular helper T (TFH) cells. *Blood.* 2007;109(11):4952-4963.
4. Gaulard P, de Leval L. Pathology of peripheral T-cell lymphomas: where do we stand? *Semin Hematol.* 2014;51(1):5-16.
5. Dobay MP, Lemonnier F, Missiaglia E, et al. A PTCL, NOS subset with molecular and clinical features similar to AITL. *Hematol Oncol.* 2015;33(S1):100-180.
6. Mourad N, Mounier N, Brière J, et al; Groupe d'Etude des Lymphomes de l'Adulte. Clinical, biologic, and pathologic features in 157 patients with angioimmunoblastic T-cell lymphoma treated within the Groupe d'Etude des Lymphomes de l'Adulte (GELA) trials. *Blood.* 2008;111(9):4463-4470.
7. Corradini P, Vitolo U, Rambaldi A, et al. Intensified chemo-immunotherapy with or without stem cell transplantation in newly diagnosed patients with peripheral T-cell lymphoma. *Leukemia.* 2014;28(9):1885-1891.
8. Lemonnier F, Couronné L, Parrens M, et al. Recurrent TET2 mutations in peripheral T-cell lymphomas correlate with TFH-like features and adverse clinical parameters. *Blood.* 2012;120(7):1466-1469.
9. Cairns RA, Iqbal J, Lemonnier F, et al. IDH2 mutations are frequent in angioimmunoblastic T-cell lymphoma. *Blood.* 2012;119(8):1901-1903.
10. Jaiswal S, Fontanillas P, Flannick J, et al. Age-related clonal hematopoiesis associated with adverse outcomes. *N Engl J Med.* 2014;371(26):2488-2498.
11. Muto H, Sakata-Yanagimoto M, Nagae G, et al. Reduced TET2 function leads to T-cell lymphoma with follicular helper T-cell-like features in mice. *Blood Cancer J.* 2014;4(12):e264.
12. Palomero T, Couronné L, Khiabanian H, et al. Recurrent mutations in epigenetic regulators, RHOA and FYN kinase in peripheral T cell lymphomas. *Nat Genet.* 2014;46(2):166-170.
13. Sakata-Yanagimoto M, Enami T, Yoshida K, et al. Somatic RHOA mutation in angioimmunoblastic T cell lymphoma. *Nat Genet.* 2014;46(2):171-175.
14. Yoo HY, Sung MK, Lee SH, et al. A recurrent inactivating mutation in RHOA GTPase in angioimmunoblastic T cell lymphoma. *Nat Genet.* 2014;46(4):371-375.
15. Cleverley SC, Costello PS, Henning SW, Cantrell DA. Loss of Rho function in the thymus is accompanied by the development of thymic lymphoma. *Oncogene.* 2000;19(1):13-20.
16. Odejide O, Weigert O, Lane AA, et al. A targeted mutational landscape of angioimmunoblastic T-cell lymphoma. *Blood.* 2014;123(9):1293-1296.
17. Wilson WH, Young RM, Schmitz R, et al. Targeting B cell receptor signaling with ibrutinib in diffuse large B cell lymphoma. *Nat Med.* 2015;21(8):922-926.
18. Inghirami G, Chan WC, Pileri S; AIRC 5xMille consortium 'Genetics-driven targeted management of lymphoid malignancies'. Peripheral T-cell and NK cell lymphoproliferative disorders: cell of origin, clinical and pathological implications. *Immunol Rev.* 2015;263(1):124-159.
19. Pechloff K, Holch J, Ferch U, et al. The fusion kinase ITK-SYK mimics a T cell receptor signal and drives oncogenesis in conditional mouse models of peripheral T cell lymphoma. *J Exp Med.* 2010;207(5):1031-1044.
20. Kataoka K, Nagata Y, Kitanaka A, et al. Integrated molecular analysis of adult T cell leukemia/lymphoma. *Nat Genet.* 2015;47(11):1304-1315.
21. Vaqué JP, Gómez-López G, Monsálvez V, et al. PLCG1 mutations in cutaneous T-cell lymphomas. *Blood.* 2014;123(13):2034-2043.
22. Manso R, Rodríguez-Pinilla SM, González-Rincón J, et al. Recurrent presence of the PLCG1 S345F mutation in nodal peripheral T-cell lymphomas. *Haematologica.* 2015;100(1):e25-e27.
23. da Silva Almeida AC, Abate F, Khiabanian H, et al. The mutational landscape of cutaneous T cell lymphoma and Sézary syndrome. *Nat Genet.* 2015;47(12):1465-1470.
24. Wang L, Ni X, Covington KR, et al. Genomic profiling of Sézary syndrome identifies alterations of key T cell signaling and differentiation genes. *Nat Genet.* 2015;47(12):1426-1434.
25. Rohr J, Guo S, Huo J, et al. Recurrent activating mutations of CD28 in peripheral T-cell lymphomas. *Leukemia.* 2016;30(5):1062-1070.
26. Morin RD, Mendez-Lago M, Mungall AJ, et al. Frequent mutation of histone-modifying genes in non-Hodgkin lymphoma. *Nature.* 2011;476(7360):298-303.
27. Lenz G, Davis RE, Ngo VN, et al. Oncogenic CARD11 mutations in human diffuse large B cell lymphoma. *Science.* 2008;319(5870):1676-1679.
28. Pelzer C, Cabalzar K, Wolf A, Gonzalez M, Lenz G, Thome M. The protease activity of the paracaspase MALT1 is controlled by monoubiquitination. *Nat Immunol.* 2013;14(4):337-345.
29. Wang D, You Y, Case SM, et al. A requirement for CARMA1 in TCR-induced NF-kappa B activation. *Nat Immunol.* 2002;3(9):830-835.
30. Lee SH, Kim JS, Kim J, et al. A highly recurrent novel missense mutation in CD28 among angioimmunoblastic T-cell lymphoma patients. *Haematologica.* 2015;100(12):e505-e507.
31. Huang C-H, Mandelker D, Schmidt-Kittler O, et al. The structure of a human p110α/p85α complex elucidates the effects of oncogenic PI3Kalpha mutations. *Science.* 2007;318(5857):1744-1748.
32. Austinat M, Dunsch R, Wittekind C, Tannapfel A, Gebhardt R, Gaunitz F. Correlation between β-catenin mutations and expression of Wnt-signaling target genes in hepatocellular carcinoma. *Mol Cancer.* 2008;7(1):21.
33. Pilati C, Letouzé E, Nault J-C, et al. Genomic profiling of hepatocellular adenomas reveals recurrent FRK-activating mutations and the mechanisms of malignant transformation. *Cancer Cell.* 2014;25(4):428-441.
34. Stolze B, Reinhart S, Bulllinger L, Fröhling S, Scholl C. Comparative analysis of KRAS codon 12, 13, 18, 61, and 117 mutations using human MCF10A isogenic cell lines. *Sci Rep.* 2015;5:8535.
35. Ohgami RS, Ma L, Monabati A, Zehnder JL, Arber DA. STAT3 mutations are present in aggressive B-cell lymphomas including a subset of diffuse large B-cell lymphomas with CD30 expression. *Haematologica.* 2014;99(7):e105-e107.
36. Nagata Y, Kontani K, Enami T, et al. Variegated RHOA mutations in adult T-cell leukemia/lymphoma. *Blood.* 2016;127(5):596-604.
37. Koskela HL, Eldfors S, Ellonen P, et al. Somatic STAT3 mutations in large granular lymphocytic leukemia. *N Engl J Med.* 2012;366(20):1905-1913.
38. Jerez A, Clemente MJ, Makishima H, et al. STAT3 mutations unify the pathogenesis of chronic lymphoproliferative disorders of NK cells and T-cell large granular lymphocyte leukemia. *Blood.* 2012;120(15):3048-3057.
39. Koo GC, Tan SY, Tang T, et al. Janus kinase 3-activating mutations identified in natural killer/T-cell lymphoma. *Cancer Discov.* 2012;2(7):591-597.
40. Kiel MJ, Velusamy T, Rolland D, et al. Integrated genomic sequencing reveals mutational landscape of T-cell prolymphocytic leukemia. *Blood.* 2014;124(9):1460-1472.
41. Bellanger D, Jacquemin V, Chopin M, et al. Recurrent JAK1 and JAK3 somatic mutations in T-cell prolymphocytic leukemia. *Leukemia.* 2014;28(2):417-419.
42. Nicolae A, Xi L, Pittaluga S, et al. Frequent STAT5B mutations in γδ hepatosplenic T-cell lymphomas. *Leukemia.* 2014;28(11):2244-2248.
43. Küçük C, Jiang B, Hu X, et al. Activating mutations of STAT5B and STAT3 in lymphomas derived from γδ-T or NK cells. *Nat Commun.* 2015;6:6025.
44. Avbelj M, Wolz O-O, Fekonja O, et al. Activation of lymphoma-associated MyD88 mutations via allostery-induced TIR-domain oligomerization. *Blood.* 2014;124(26):3896-3904.
45. Ihara K, Muraguchi S, Kato M, et al. Crystal structure of human RhoA in a dominantly active form complexed with a GTP analogue. *J Biol Chem.* 1998;273(16):9656-9666.
46. Laham LE, Mukhopadhyay N, Roberts TM. The activation loop in Lck regulates oncogenic potential by inhibiting basal kinase activity and restricting substrate specificity. *Oncogene.* 2000;19(35):3961-3970.
47. Chinen Y, Kuroda J, Shimura Y, et al. Phosphoinositide protein kinase PDPK1 is a crucial cell signaling mediator in multiple myeloma. *Cancer Res.* 2014;74(24):7418-7429.
48. Sacristán C, Schattgen SA, Berg LJ, Bunnell SC, Roy AL, Rosenstein Y. Characterization of a novel interaction between transcription factor TFII-I and the inducible tyrosine kinase

in T cells. *Eur J Immunol*. 2009;39(9):2584-2595.

49. Petrini I, Meltzer PS, Kim I-K, et al. A specific missense mutation in GTF2I occurs at high frequency in thymic epithelial tumors. *Nat Genet*. 2014;46(8):844-849.

50. Razanadrakoto L, Cormier F, Laurienté V, et al. Mutation of Vav1 adaptor region reveals a new oncogenic activation. *Oncotarget*. 2015;6(4):2524-2537.

51. Singh NJ, Schwartz RH. The strength of persistent antigenic stimulation modulates adaptive tolerance in peripheral CD4+ T cells. *J Exp Med*. 2003;198(7):1107-1117.

52. Ishikawa S. Opposite RHOA functions within the ATLL category. *Blood*. 2016;127(5):524-525.

53. Kiel MJ, Sahasrabuddhe AA, Rolland DCM, et al. Genomic analyses reveal recurrent mutations in epigenetic modifiers and the JAK-STAT pathway in Sézary syndrome. *Nat Commun*. 2015;6:8470.

54. Wang C, McKeithan TW, Gong Q, et al. IDH2R172 mutations define a unique subgroup of patients with angioimmunoblastic T-cell lymphoma. *Blood*. 2015;126(15):1741-1752.

55. Sakata-Yanagimoto M. Multistep tumorigenesis in peripheral T cell lymphoma. *Int J Hematol*. 2015;102(5):523-527.

56. Quivoron C, Couronné L, Della Valle V, et al. TET2 inactivation results in pleiotropic hematopoietic abnormalities in mouse and is a recurrent event during human lymphomagenesis. *Cancer Cell*. 2011;20(1):25-38.

57. Cheminant M, Bruneau J, Kosmider O, et al. Efficacy of 5-azacytidine in a TET2 mutated angioimmunoblastic T cell lymphoma. *Br J Haematol*. 2015;168(6):913-916.

2016 128: 1490-1502
doi:10.1182/blood-2016-02-698977 originally published online July 1, 2016

Activating mutations in genes related to TCR signaling in angioimmunoblastic and other follicular helper T-cell–derived lymphomas

David Vallois, Maria Pamela D. Dobay, Ryan D. Morin, François Lemonnier, Edoardo Missiaglia, Mélanie Juilland, Justyna Iwaszkiewicz, Virginie Fataccioli, Bettina Bisig, Annalisa Roberti, Jasleen Grewal, Julie Bruneau, Bettina Fabiani, Antoine Martin, Christophe Bonnet, Olivier Michielin, Jean-Philippe Jais, Martin Figeac, Olivier A. Bernard, Mauro Delorenzi, Corinne Haioun, Olivier Tournilhac, Margot Thome, Randy D. Gascoyne, Philippe Gaulard and Laurence de Leval

Blood (print ISSN 0006-4971, online ISSN 1528-0020), is published weekly by the American Society of Hematology, 2021 L St, NW, Suite 900, Washington DC 20036.